

# Olfactory receptor and circuit evolution promote host specialization

<https://doi.org/10.1038/s41586-020-2073-7>

Received: 13 February 2019

Accepted: 31 January 2020

Published online: 4 March 2020

 Check for updates

Thomas O. Auer<sup>1✉</sup>, Mohammed A. Khallaf<sup>2</sup>, Ana F. Silbering<sup>1</sup>, Giovanna Zappia<sup>1</sup>, Kaitlyn Ellis<sup>3</sup>, Raquel Álvarez-Ocaña<sup>1</sup>, J. Roman Arguello<sup>4</sup>, Bill S. Hansson<sup>2</sup>, Gregory S. X. E. Jefferis<sup>5</sup>, Sophie J. C. Caron<sup>5</sup>, Markus Knaden<sup>2</sup> & Richard Benton<sup>1✉</sup>

The evolution of animal behaviour is poorly understood<sup>1,2</sup>. Despite numerous correlations between interspecific divergence in behaviour and nervous system structure and function, demonstrations of the genetic basis of these behavioural differences remain rare<sup>3–5</sup>. Here we develop a neurogenetic model, *Drosophila sechellia*, a species that displays marked differences in behaviour compared to its close cousin *Drosophila melanogaster*<sup>6,7</sup>, which are linked to its extreme specialization on noni fruit (*Morinda citrifolia*)<sup>8–16</sup>. Using calcium imaging, we identify olfactory pathways in *D. sechellia* that detect volatiles emitted by the noni host. Our mutational analysis indicates roles for different olfactory receptors in long- and short-range attraction to noni, and our cross-species allele-transfer experiments demonstrate that the tuning of one of these receptors is important for species-specific host-seeking. We identify the molecular determinants of this functional change, and characterize their evolutionary origin and behavioural importance. We perform circuit tracing in the *D. sechellia* brain, and find that receptor adaptations are accompanied by increased sensory pooling onto interneurons as well as species-specific central projection patterns. This work reveals an accumulation of molecular, physiological and anatomical traits that are linked to behavioural divergence between species, and defines a model for investigating speciation and the evolution of the nervous system.

The genetic and neural basis by which animals adapt behaviourally to their ecological niche is largely unknown<sup>1,2</sup>. Insights have previously been gained from investigating intraspecific variation in traditional model organisms, including anxiety behaviours in *Mus musculus*<sup>17</sup> and exploration versus exploitation decisions in *Caenorhabditis elegans*<sup>18</sup>. Interspecific differences are more marked than intraspecific differences. For example, distinct species of *Peromyscus* mice display variations in burrowing and parental care<sup>3,5</sup>, and the predatory nematode *Pristionchus pacificus* exhibits feeding behaviours that are divergent from those of *C. elegans*<sup>19</sup>. Defining the molecular basis of interspecific differences is challenging as it requires both that species are comparable in molecular and anatomical terms, and that they can be genetically manipulated.

Drosophilid flies are attractive models for investigating behavioural evolution: *D. melanogaster* offers deep neurobiological knowledge in a numerically relatively simple brain, and closely related drosophilid species show distinct behaviours that are linked to their diverse ecologies<sup>20</sup>. Several of these behavioural traits have previously been correlated to anatomical and/or physiological changes in sensory or central pathways<sup>4,11,13,15,21,22</sup>. One notable drosophilid is *D. sechellia*, which is endemic to the Seychelles and shares a recent common ancestor with the cosmopolitan ecological generalists *D. melanogaster*

and *Drosophila simulans*<sup>6,7</sup> (Fig. 1a). *D. sechellia* has evolved extreme specialism for noni fruit (Fig. 1a), and displays olfactory<sup>11–13,15,16</sup>, gustatory<sup>14</sup> and reproductive behaviours<sup>8–10</sup> that are unique among known drosophilids. Mapping approaches have located causal loci for some traits specific to *D. sechellia* (typically within large genomic regions<sup>8,10</sup>), and candidate approaches have correlated chemosensory phenotypes with changes in the peripheral sensory pathways of this species<sup>11,14,15</sup>.

Despite the potential that *D. sechellia* presents for comparative neuroscience, investigations of the behaviours of *D. sechellia* have been limited by a lack of genetic tools. Here we develop *D. sechellia* into a genetic model system, moving from genotypic–phenotypic correlations to test the role of genetic changes in behavioural evolution.

## Specific noni attraction of *D. sechellia*

Noni-derived volatiles are probably the initial cues that guide *D. sechellia* host-seeking<sup>16</sup>. We used two assays to compare the attraction of wild-type strains of *D. sechellia*, *D. simulans* and *D. melanogaster* to noni at distinct spatial scales (Fig. 1b, c, Extended Data Fig. 1). In a long-range wind tunnel assay<sup>23</sup>, *D. sechellia* displayed a higher attraction to noni than that of its sister species (Fig. 1b); in a short-range trap assay<sup>15</sup>, only *D. sechellia* exhibits a marked preference for noni (Fig. 1c).

<sup>1</sup>Center for Integrative Genomics, Faculty of Biology and Medicine, University of Lausanne, Lausanne, Switzerland. <sup>2</sup>Department of Evolutionary Neuroethology, Max Planck Institute for Chemical Ecology, Jena, Germany. <sup>3</sup>Department of Biology, University of Utah, Salt Lake City, UT, USA. <sup>4</sup>Department of Ecology and Evolution, Faculty of Biology and Medicine, University of Lausanne, Lausanne, Switzerland. <sup>5</sup>Division of Neurobiology, MRC Laboratory of Molecular Biology, Cambridge, UK. ✉e-mail: Thomas.Auer@unil.ch; Richard.Benton@unil.ch

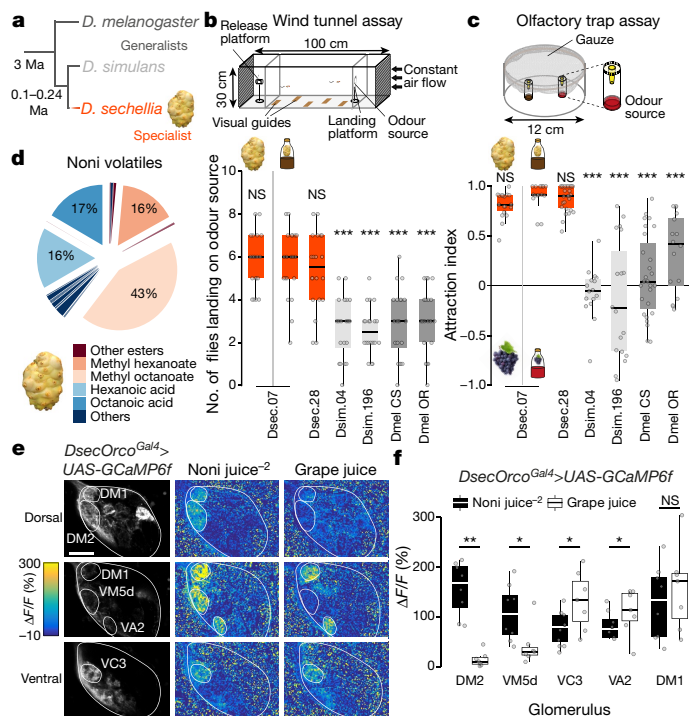


**Fig. 1 Behavioural and physiological responses of *D. sechellia* to noni.**  
**a**, *D. sechellia* specializes on noni fruit, whereas *D. simulans* and *D. melanogaster* are food generalists. Ma, million years ago. **b**, Behavioural responses to noni fruit or juice in a wind tunnel assay of *D. sechellia*, *D. simulans* and *D. melanogaster* wild-type strains ( $n = 20$  experiments, with 10 female flies per experiment). Comparisons to the responses of *D. sechellia* 14021-0248.07 flies (Dsec.07) (Supplementary Table 2 provides details of fly strains) to noni juice are shown. Kruskal–Wallis test, Dunn’s post hoc correction. **c**, Behavioural responses in a trap assay testing preferences between noni and grape or between noni juice and grape juice, using the same strains as in **b**.  $n = 15–27$  experiments, 22–25 female flies per experiment (exact  $n$  values are given in the Source Data). Comparisons to the responses of Dsec.07 flies to noni juice are shown. Pairwise Wilcoxon rank-sum test,  $P$  values adjusted for multiple comparisons using the Benjamini and Hochberg method. **d**, Odour bouquet of a ripe noni fruit determined by gas chromatography–mass spectrometry (Extended Data Fig. 2, Methods, Supplementary Table 1). **e**, Representative odour-evoked calcium responses in the axon termini of Orco OSNs in the *D. sechellia* antennal lobe (genotype *UAS-GCaMP6f/UAS-GCaMP6f;DsecOrco<sup>Gal4/+</sup>*) acquired by two-photon imaging. Three focal planes are shown, revealing different glomeruli (outlined) along the dorsoventral axis. Left, raw fluorescence images. Right and middle, relative increase in GCaMP6f fluorescence ( $\Delta F/F\%$ ) after stimulation with noni juice ( $10^{-2}$  dilution in  $H_2O$ ; denoted noni juice<sup>-2</sup>) or grape juice. Scale bar, 25  $\mu m$ . **f**, Quantification of responses for the flies represented in **e**. Maximum response amplitudes for each experiment are plotted.  $n = 7–10$  female flies. Wilcoxon signed-rank test. All box plots show the median and first and third quartiles of the data, overlaid with individual data points. NS, not significant ( $P > 0.05$ ); \* $P < 0.05$ ; \*\* $P < 0.01$ ; \*\*\* $P < 0.001$ .

The behaviour of this species towards noni juice (which represents an odour stimulus that is more reproducible than that of noni fruit) was comparable to that for ripe fruit (Fig. 1b, c), concordant with their qualitatively similar odour bouquets (Fig. 1d, Extended Data Fig. 2a, b, Methods). Assays using other natural odour sources, as previously described in field studies<sup>24</sup>, confirmed the unique attractiveness of noni for *D. sechellia* (Extended Data Fig. 1a–e, g).

### Noni-sensing olfactory pathways

Drosophilids detect odours using olfactory sensory neurons (OSNs) in sensilla on their antennae and maxillary palps<sup>25</sup>. Most OSNs express a

single odour receptor (Or) or ionotropic receptor (Ir)—which defines odour-tuning properties—along with an obligate co-receptor<sup>26–28</sup>. Neurons that express the same tuning receptor converge onto a discrete glomerulus in the antennal lobe<sup>25</sup>. Previous electrophysiological analyses in *D. sechellia* have identified several OSN populations that respond to individual noni odours<sup>11,13,15,29</sup>, but the global representation of the noni bouquet has not been examined.

We generated transgenic *D. sechellia* that express GCaMP6f in the majority of OSNs, under the control of *Gal4* inserted at the *Or co-receptor* (*DsecOrco*) locus (Extended Data Fig. 3). Using wide-field imaging to compare this and an equivalent *D. melanogaster* line (Extended Data Fig. 4a), we did not detect noni-responsive olfactory channels unique to *D. sechellia* but instead found quantitative differences in individual glomerular responses between species (Extended Data Fig. 4b). Two-photon calcium imaging highlighted two glomeruli (DM2 and VM5d) that are distinguished by their very high sensitivity to noni compared to grape juice in *D. sechellia* (Fig. 1e, f, Extended Data Fig. 4b–d). These glomeruli are innervated by OSNs that are housed in the same antennal basiconic sensillum class (ab3) and that respond electrophysiologically to individual noni odours<sup>11,13</sup>.

### Genetic targeting of olfactory receptors

We determined the electrophysiological responses of noni-sensitive olfactory channels to a range of noni odours (Fig. 2a, b, Extended Data Figs. 4e, 5, 6), and mutated candidate olfactory receptors (Extended Data Figs. 5, 6). In wild-type ab3 sensilla, the larger-spiking ab3A neuron responded most strongly to methyl esters and the smaller-spiking ab3B neuron was highly stimulated by 2-heptanone and 1-hexanol (Fig. 2a). All of these responses were lost in *DsecOrco* mutants, (Fig. 2a), which indicates that these responses are dependent on Or signalling.

The *D. melanogaster* ab3A neuron expresses the *Or22a* and *Or22b* genes<sup>30</sup>, whereas *D. sechellia* possesses only *DsecOr22a*<sup>11</sup>. Targeted mutation of this latter locus abolished the odour-evoked responses of the ab3A, but not the ab3B, neuron (Fig. 2a). The receptor in the *D. melanogaster* ab3B neuron is thought to be *Or85b*<sup>25,31</sup>, but *D. sechellia* neurons with a mutation in *DsecOr85b* retained some sensitivity to noni odours (Fig. 2a). Deletion of *DsecOr85b* and the neighbouring *DsecOr85c*—transcripts of which have previously been detected in an antennal transcriptome<sup>32</sup>—led to complete loss of responses of ab3B neurons, arguing for partial receptor redundancy (Fig. 2a).

In *D. sechellia*, Ir75b neurons in antennal coeloconic 3I (ac3I) sensilla have evolved a sensitivity to hexanoic acid that does not exist in *D. melanogaster* or *D. simulans*<sup>15</sup>. Mutations in *DsecIr75b* or *DsecIr8a* (which encodes an Ir co-receptor<sup>27</sup>) led to a selective loss of responses to hexanoic acid and butyric acid in the ac3I sensillum (Fig. 2b, Extended Data Fig. 6). Mutation of *DsecOr35a* (expressed in the paired neuron) diminished responses to all odours except these acids, consistent with the broad tuning of this receptor in *D. melanogaster*<sup>33</sup>.

### Odorant receptors for long-range attraction

We used the receptor mutants to determine the behavioural role of individual olfactory pathways. In the long-range assay, *DsecOrco* mutants exhibited no attraction to the odour source (Fig. 2c). Notably, flies with a mutation in *DsecOr22a* or in *DsecOr85c* and *DsecOr85b* (hereafter, *DsecOr85c/b*) both displayed similar, strong defects (Fig. 2c). By contrast, *DsecOr35a* mutants were not impaired (Fig. 2c). Loss of Ir8a also led to a significant decrease in long-range attraction in *D. sechellia* (Fig. 2c). This does not appear to be primarily due to defects in the hexanoic-acid-sensing pathway, as *DsecIr75b* mutants had either no or milder defects than *DsecIr8a* mutants (Fig. 2c). Loss of *DsecIr64a*—which is broadly tuned to acids in *D. melanogaster*<sup>34</sup>, and responded to noni in *D. sechellia* (Extended Data Fig. 4f, g)—had no effect on this behaviour.

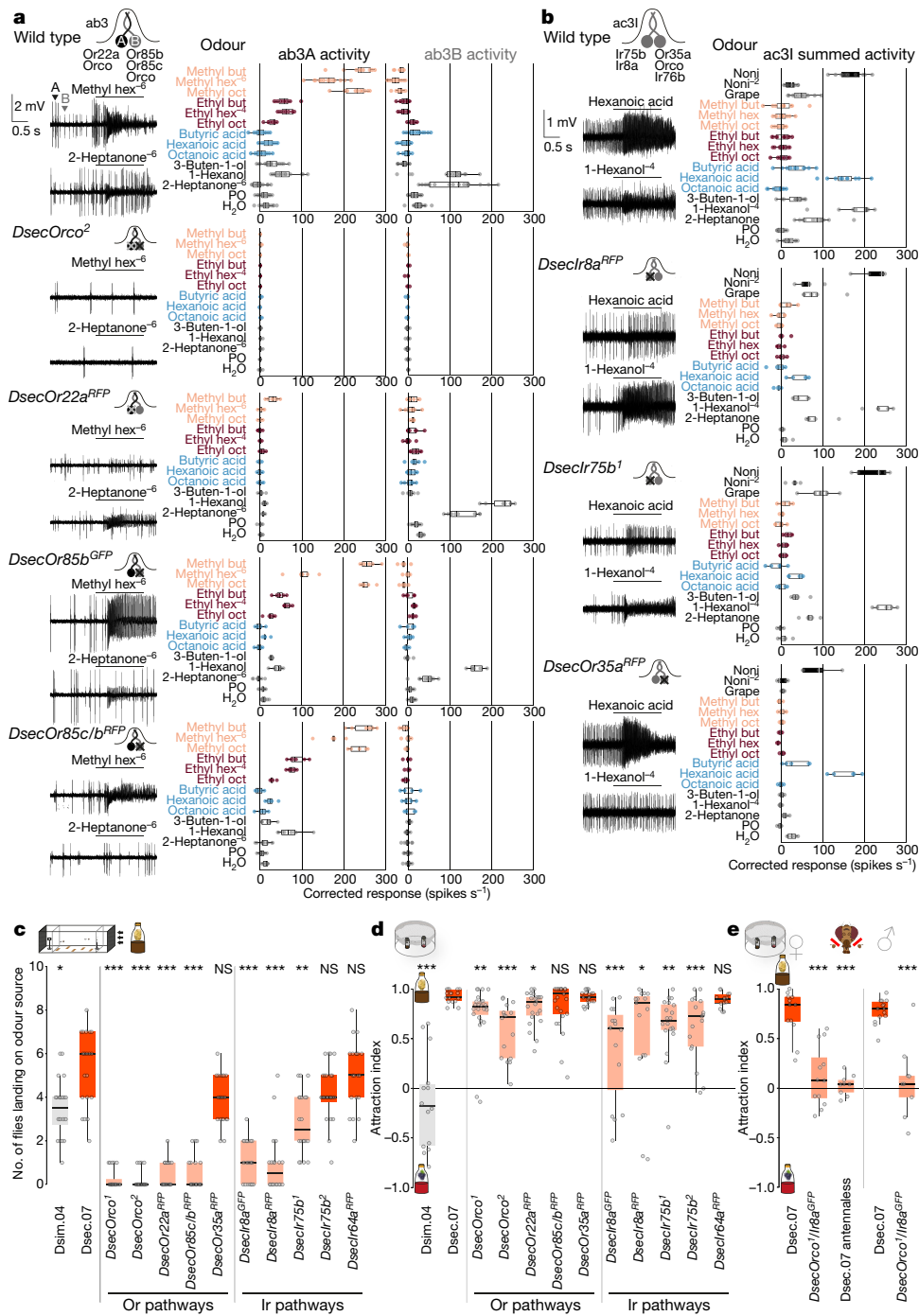


**Fig. 2 | Olfactory receptor contributions to noni-sensing.**

**a**, Electrophysiological responses of neurons of the *ab3* sensillum to noni odours ( $n = 5-20$ , female flies, Supplementary Table 7 provides exact  $n$  values and mean spike counts) in wild-type and receptor-mutant *D. sechellia* (schematized in the cartoons), with representative traces for methyl hexanoate (hex) and 2-heptanone. Data points are the solvent-corrected activities of individual neurons (arrowheads in the wild-type trace). Odours are coloured according to chemical class: methyl esters (salmon), ethyl esters (dark red), acids (light blue) and others (black). Odorants were used at  $10^{-2}$  dilution (v/v) in double-distilled water or paraffin oil (PO) (see ‘Electrophysiology’ in the Methods for details), unless indicated otherwise in superscript (for example, methyl hex<sup>-6</sup> denotes methyl hexanoate at  $10^{-6}$  dilution (v/v)). But, butanoate; hex, hexanoate; oct, octanoate. **b**, Responses of neurons of the *ac31* sensillum to noni juice, grape juice and noni odours ( $n = 5-11$ , female flies) in wild-type and receptor-mutant *D. sechellia*, with representative traces for

hexanoic acid and 1-hexanol. Data points are the summed solvent-corrected activities of both neurons. **c**, Behavioural responses to noni juice in the wind tunnel assay ( $n = 20$  experiments). Comparisons to the response of *Dsec.07* flies are shown. Kruskal–Wallis test, Dunn’s post hoc correction. In **c–e**, red denotes no significant difference, and salmon denotes a significantly different responses of the *D. sechellia* genotypes. **d**, Behavioural responses in the trap assay testing preference for noni juice or grape juice ( $n = 13-25$  experiments). Comparisons to responses of *Dsec.07* flies are shown. **e**, Behavioural responses in the trap assay testing preference for noni juice or grape juice, using wild-type *D. sechellia*, *DsecOrco1 Ir8a<sup>GFP</sup>* double mutants and antennaless *D. sechellia* ( $n = 9-15$  experiments, 22–25 female or male (as indicated) flies per experiment). Average attraction indices for *DsecOrco1 Ir8a<sup>GFP</sup>* and antennaless flies are not significantly different from zero. In **d, e**, pairwise Wilcoxon rank-sum test,  $P$  values adjusted for multiple comparisons using the Benjamini and Hochberg method. NS, not significant ( $P > 0.05$ ); \* $P < 0.05$ ; \*\* $P < 0.01$ ; \*\*\* $P < 0.001$ .



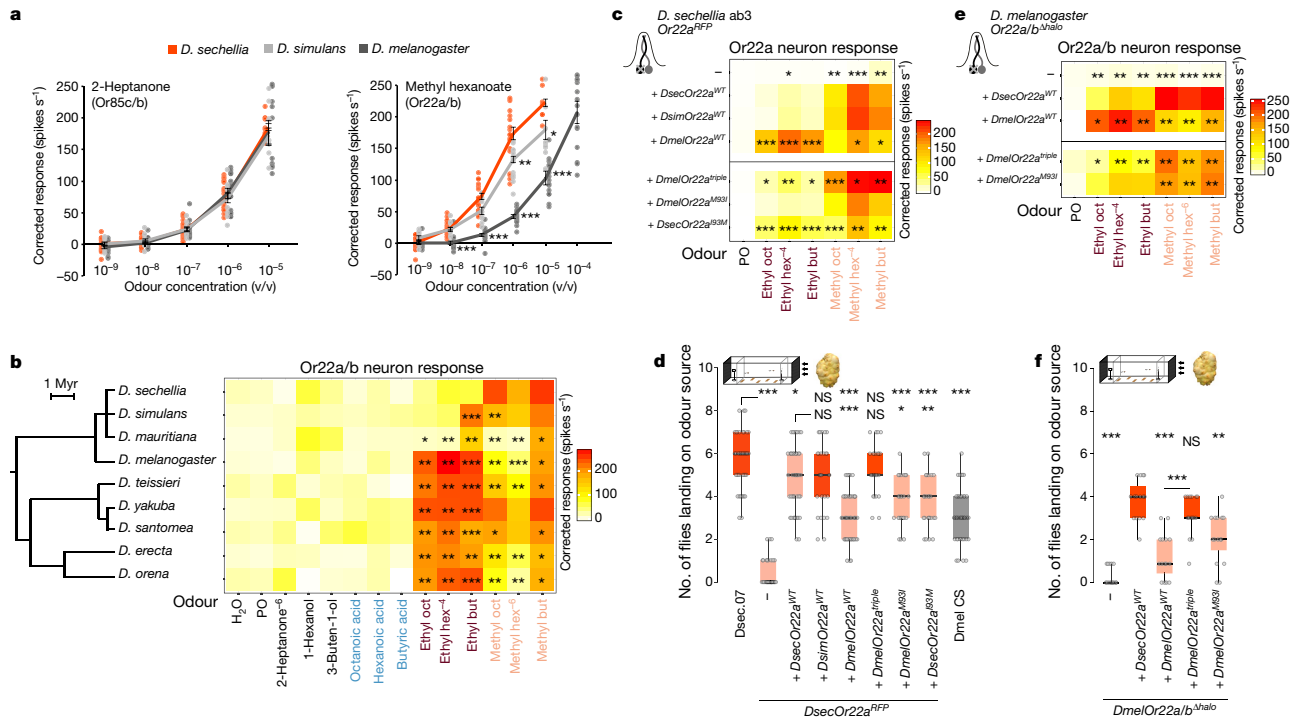


**Fig. 3 | Tuning of Or22a is important for attraction to noni.**

**a**, Dose-dependent responses of Or85c/b (left) and Or22a/b (right) neurons in Dsec.07, Dsim.04 and Dmel CS to 2-heptanone and methyl hexanoate, respectively. Mean  $\pm$  s.e.m. and individual data points;  $n = 5-20$ , female flies. Significant differences to responses of *D. sechellia* are shown. In **a-c**, pairwise Wilcoxon rank-sum test, *P* values adjusted for multiple comparisons using the Benjamini and Hochberg method. **b**, Responses of Or22a/b neurons to noni odours across the *D. melanogaster* species subgroup of drosophilids. In all instances, 'D.' denotes *Drosophila*. Myr, million years.  $n = 5-20$ , female flies. Data for *D. sechellia* responses are replotted from Fig. 2a. Significant differences to responses of *D. sechellia* to esters are shown. **c**, Responses of Or22a neurons from *D. sechellia* expressing wild-type (top) or mutant (bottom) versions of Or22a inserted at the Or22a locus ( $n = 10-18$ , female flies). Significant differences to the responses of DsecOr22a<sup>WT</sup> flies are shown (c, e). Responses to methyl hexanoate are a 10<sup>-4</sup> dilution (v/v) in this panel compared

with a 10<sup>-6</sup> dilution in **b**, **e**. Superscript 'triple' denotes mutations that give rise to Or22a(145V/167M/M93I). **d**, Behavioural responses to noni fruit in the wind tunnel assay.  $n = 25-45$  experiments. Comparisons to responses of Dsec.07 (top line of *P* values) and DsecOr22a<sup>WT</sup> (bottom line of *P* values) flies responses are shown. In **d**, **f**, Kruskal-Wallis test, Dunn's post hoc correction. Salmon, *D. sechellia* genotypes with significantly different responses to that of Dsec.07 flies. **e**, Responses of *D. melanogaster* Or22a/b-mutant neurons expressing wild-type (top) or mutant (bottom) versions of Or22a.  $n = 5-7$ , female flies. Box plots of data in **b**, **c**, **e** are shown in Extended Data Fig. 8g, h, i, respectively. **f**, Behavioural responses to noni fruit in the wind tunnel assay.  $n = 20$  experiments. Comparisons to responses of DsecOr22a<sup>WT</sup> (top line of *P* values) and DmelOr22a<sup>WT</sup> (bottom line of *P* values) flies are shown. Salmon, genotypes with significantly different responses to that of DsecOr22a<sup>WT</sup> flies. NS, not significant ( $P > 0.05$ ); \* $P < 0.05$ ; \*\* $P < 0.01$ ; \*\*\* $P < 0.001$ .

In the short-range assay, DsecOrco mutants displayed a reduced, but not abolished, preference for noni (Fig. 2d). Flies with mutations in individual Or pathways had very slight (DsecOr22a) or no (DsecOr85c/b and DsecOr35a) defects in this behaviour (Fig. 2d, Extended Data Fig. 7). DsecOr8a or DsecOr75b (but not DsecOr64a) mutants displayed a reduced preference for noni, with notable frequent preference reversals in several trials (Fig. 2d). Flies with mutations in both DsecOrco and DsecOr8a, as well as antennaless flies, displayed no noni preference (Fig. 2e, Extended Data Fig. 7c, d), indicating that this short-range behaviour depends on multiple partially redundant olfactory inputs. Consistent with these observations, individual noni odours promoted a strong preference at short range, whereas they triggered no or little flight attraction at long range<sup>11,13,15</sup> (Extended Data Fig. 7f, g). The relative contribution of individual channels to these behaviours may be related to their detection thresholds (Extended Data Fig. 2c) and/or differential diffusion of cognate odours within each assay (Extended Data Fig. 2d, e).

### Tuning of Or22a affects behaviour

Given the crucial role of Or22a and Or85c/b in long-range attraction, we explored the evolution of these pathways. Or85c/b neurons displayed an indistinguishable sensitivity across species to their best agonist, 2-heptanone. By contrast, Or22a neurons of *D. sechellia*, and

Or22a and Or22b (hereafter, Or22a/b) neurons of *D. simulans*, exhibited increased sensitivity to methyl hexanoate, compared to that of *D. melanogaster*<sup>11,29</sup> (Fig. 3a, Extended Data Fig. 8a). Broader profiling of Or22a/b neurons in the *D. melanogaster* species subgroup of drosophilids (Fig. 3b, Extended Data Fig. 8g) revealed that *D. sechellia* was the only species with selective and high sensitivity to methyl esters; other species—including *D. simulans*—also responded to ethyl esters (Fig. 3b). This suggests that changes in the tuning sensitivity and/or breadth of Or22a (but not Or85c/b) contribute to the differences in behaviour of *D. sechellia* relative to *D. melanogaster*.

We next reintroduced wild-type DsecOr22a (DsecOr22a<sup>WT</sup>), DsimOr22a<sup>WT</sup> or DmelOr22a<sup>WT</sup> into the DsecOr22a endogenous locus (Extended Data Fig. 8b). Expression of DsecOr22a<sup>WT</sup> or DmelOr22a<sup>WT</sup> restored electrophysiological-response profiles similar to those of the native neuronal responses, indicating that the receptor is key for the species-specific tuning of neurons (Fig. 3c top). Introducing DsimOr22a<sup>WT</sup> conferred sensitivity to methyl esters, but not to ethyl esters (Fig. 3b, c, Extended Data Fig. 8h); genetic analysis in *D. simulans* indicated that the detection of ethyl esters by the endogenous Or22a/b neurons depends on the coexpressed Or22b (Extended Data Fig. 8c-f).

Concordant with their physiological properties, DsecOr22a<sup>WT</sup> and DsimOr22a<sup>WT</sup>—but not DmelOr22a<sup>WT</sup>—rescued long-range behavioural responses to almost wild-type levels (Fig. 3d). Reciprocally, the expression of DsecOr22a<sup>WT</sup> in the neurons of *D. melanogaster* flies with Or22a/b



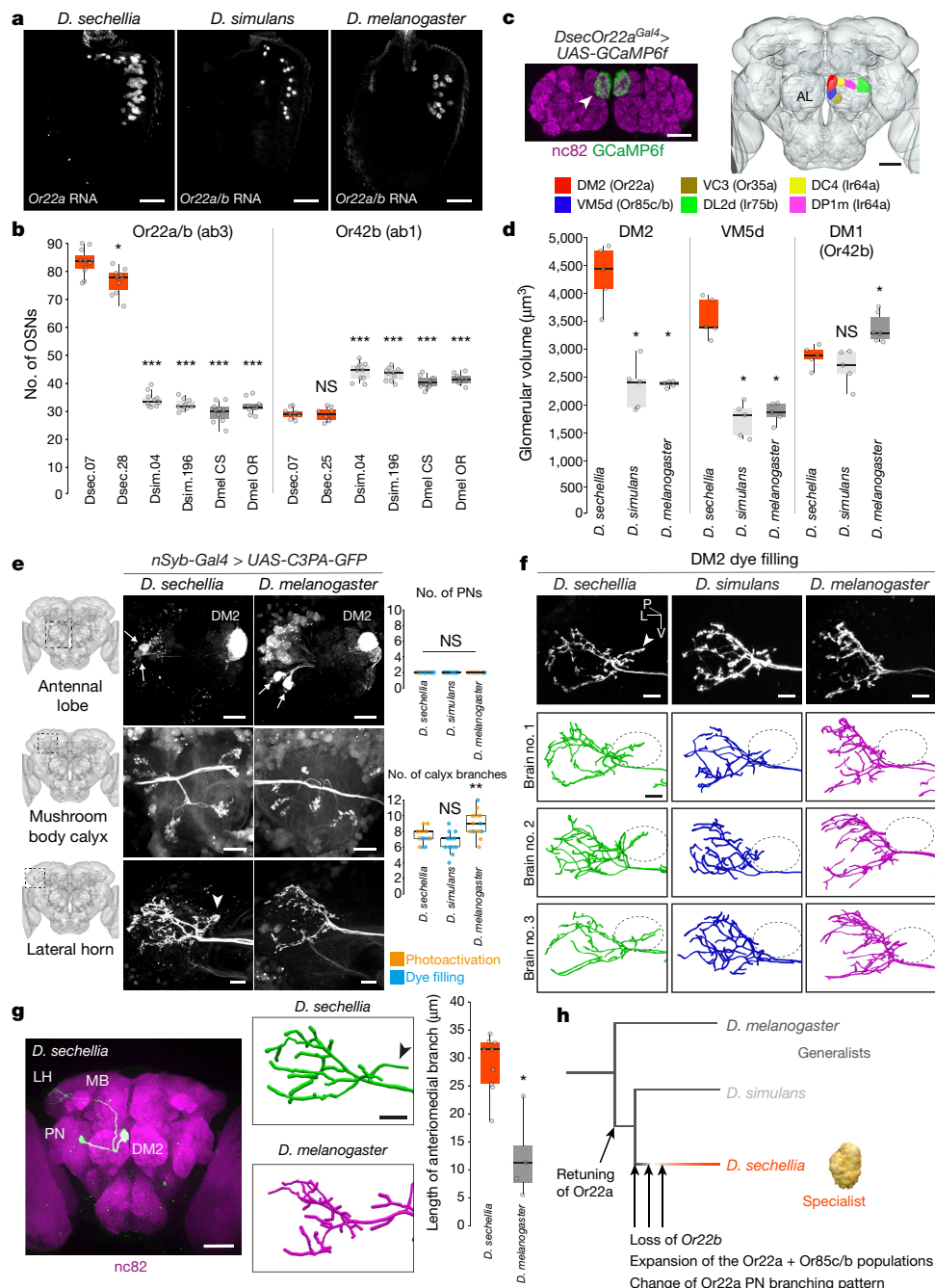


**Fig. 4 | Neuroanatomy of noni-sensing olfactory pathways.** **a**, Antennal *Or22a/b* RNA expression in different species. Scale bars, 25  $\mu$ m. **b**, Quantification of *Or22a/b* or *Or42b* OSNs.  $n = 8-11$ , female flies. Comparisons to *Dsec.07* flies are shown. In **b**, **d**, **e**, pairwise Wilcoxon rank-sum test,  $P$  values adjusted for multiple comparisons using the Benjamini and Hochberg method. **c**, Left, *Or22a<sup>Gal4</sup>*-driven *GCaMP6f* expression in DM2 (arrowhead); neuropil visualized with *nc82* (magenta). Scale bar, 25  $\mu$ m. Right, antennal lobe (AL) glomerular segmentation in *D. sechellia* (Extended Data Fig. 3). Scale bar, 50  $\mu$ m. **d**, Quantification of DM2, VM5d and DM1 volumes.  $n = 5$  female flies of each species indicated. **e**, DM2 projection neurons (PNs) labelled via photoactivation in *D. sechellia* (*DsecnSyb-Gal4/UAS-C3PA-GFP*) and *D. melanogaster* (*UAS-SPA-GFP/UAS-C3PA-GFP;nSyb-Gal4/UAS-C3PA-GFP*). Left, image acquisition site. Middle two panels show antennal lobe with labelled projection neurons (arrows) and DM2 glomerulus (scale bar, 20  $\mu$ m) (top) and projection-neuron innervation of mushroom body

calyx (middle) and lateral horn (bottom). Scale bars, 10  $\mu$ m. Arrowhead in **e-g** indicates the extra anteriomedial branch in *D. sechellia*. Right, quantification of DM2 projection neurons (top) and calyx branches (bottom).  $n = 14-17$  female flies. **f**, Top row, lateral horn arbours of dye-filled DM2 projection neurons. Genotypes of *D. sechellia* and *D. melanogaster* are as in **e**; genotype of *D. simulans* is *DsimOr22a-GFPnls*. Bottom three rows, representative lateral-horn DM2 arbour traces. Ovals, location of branch specific to *D. sechellia*. P, posterior; L, lateral; V, ventral. Scale bars, 10  $\mu$ m. **g**, Left, single dye-filled DM2 projection neuron in *D. sechellia*. MB, mushroom body; LH, lateral horn. Scale bar, 50  $\mu$ m. Middle, representative lateral horn arbour traces of DM2 projection neurons in *D. sechellia* and *D. melanogaster*. Scale bar, 10  $\mu$ m. Right, quantification of anteriomedial branch length.  $n = 4-9$  female flies. Pairwise Wilcoxon rank-sum test. NS, not significant ( $P > 0.05$ ); \* $P < 0.05$ ; \*\* $P < 0.01$ ; \*\*\* $P < 0.001$ . **h**, Evolution of structural and physiological changes in the *Or22a* pathway.

mutations (Fig. 3e top) conferred higher noni sensitivity and long-range attraction than that associated with *DmelOr22a<sup>WT</sup>* (Fig. 3f, Extended Data Figs. 8i, 9a).

**Molecular basis of *Or22a* tuning changes**

We next sought the molecular basis of the differences in the tuning of *Or22a*. Expression of chimeric versions of wild-type *DsecOr22a*

and DmelOr22a in Or22a/b neurons in *D. melanogaster* (Extended Data Fig. 9c) indicated that high sensitivity and selectivity for methyl esters are determined by the N-terminal 100 amino acids of DsecOr22a (chimaera C) (Extended Data Fig. 9b, c, e). Within these amino acids, three positions (I45, I67 and M93) differ between DmelOr22a and its orthologues in species that display a narrowed tuning for methyl esters (Extended Data Fig. 9b). Exchange of these residues to produce DmelOr22a(I45V/I67M/M93I) narrowed the responsiveness to methyl esters, similar to DsecOr22a<sup>WT</sup> (Fig. 3c, e bottom, Extended Data Fig. 9d, f). Individual mutations revealed that DmelOr22a(M93I) most closely recapitulated the higher sensitivity of this receptor to methyl esters over ethyl esters (Fig. 3c, e bottom, Extended Data Fig. 9d–g). Conversely, DsecOr22a(I93M) exhibited a broadened sensitivity to both classes of ester (Fig. 3c bottom, Extended Data Fig. 9g).

In the long-range olfactory-behaviour assay, expression of DmelOr22a(I45V/I67M/M93I) in Or22a neurons of *D. sechellia* restored an attraction to noni similar to that of wild-type *D. sechellia*, whereas both DmelOr22a(M93I) and DsecOr22a(I93M) displayed levels of attraction intermediate between those of the wild-type-receptor rescues (Fig. 3d). Similarly, expression of DmelOr22a(I45V/I67M/M93I) in *D. melanogaster* conferred noni attraction at levels equivalent to those of DsecOr22a<sup>WT</sup>, and DmelOr22a(M93I) supported intermediate levels of attraction (Fig. 3f). These results provide evidence that the molecular differences in Or22a orthologues contribute to species-specific olfactory behaviours.

### Sensory representation of Or22a

The functional similarity of Or22a orthologues in *D. sechellia* and *D. simulans* (Fig. 3c, d) indicates that additional changes have occurred during the speciation of *D. sechellia*. Concordant with ab3 sensilla counts<sup>11,29</sup>, *D. sechellia* exhibits a threefold increase in the number of Or22a neurons (recapitulated in rescue experiments shown in Extended Data Fig. 10a) and the paired Or85c/b neurons, but not several other classes of neurons<sup>15</sup> (Fig. 4a, b, Extended Data Figs. 5d, 10b).

To analyse OSN projections in *D. sechellia*, we inserted *Gal4* at the corresponding receptor loci and combined these with *UAS-GCaMP6f* as an anatomical marker (Extended Data Fig. 3). Extending single-neuron dye-filling analyses<sup>11,13,15</sup>, OSN glomerular innervation patterns were indistinguishable between *D. sechellia* and *D. melanogaster* (Fig. 4c, Extended Data Fig. 3c, d). However, the glomerular targets of Or22a and Or85c/b neurons (DM2 and VM5d, respectively) were nearly doubled in volume in *D. sechellia* compared to *D. melanogaster* or *D. simulans*<sup>11,13</sup> (Fig. 4d).

### Differences in Or22a circuit wiring

To visualize higher-order elements of the Or22a pathway, we combined a pan-neuronal driver (Extended Data Fig. 10c) with a photoactivatable *GFP* transgene to selectively photolabel DM2 projection neurons. Analysis with analogous genetic reagents in *D. melanogaster*—as well as targeted electroporation of a lipophilic dye<sup>35</sup> into this glomerulus in *D. simulans*, *D. sechellia* and *D. melanogaster*—permitted cross-species comparisons. Two DM2 projection neurons were consistently labelled in all three drosophilids (Fig. 4e).

Projection neurons innervate the mushroom body (which is required for learning and memory) and the lateral horn (which is implicated in innate olfactory responses)<sup>36</sup>. Within the former, the number and arrangement of projection-neuron axonal branches were similar between species (Fig. 4e). In the lateral horn, global anatomy was conserved, with the main tract bifurcating into dorsal and ventral branches. However, dorsal to the bifurcation, *D. sechellia* DM2 projection neurons had a prominent branch innervating an area that was not targeted by the homologous *D. melanogaster* or *D. simulans* neurons (Fig. 4e, f). Using successive photo- and dye-labelling to visualize single DM2 projection neurons in *D. sechellia* and *D. melanogaster*, we confirmed

quantitatively the presence of a branch specific to *D. sechellia* (Fig. 4g); this was also detected in flies lacking a functional DsecOr22a receptor (Extended Data Fig. 10d, e), indicating its independence of sensory input. These data raise the possibility that changes in the central circuit that are specific to *D. sechellia* form part of the olfactory specialization of this species towards noni.

### Discussion

We have developed *D. sechellia* as a model to link genetic and neural-circuit changes to behaviours relevant for its ecology. The characterization of the Or22a pathway and comparison of the functional and structural properties of this circuit across closely related species provides several insights into behavioural evolution (Fig. 4h).

The *Or22a* allele-transfer experiments provide evidence that olfactory receptor tuning contributes to species-specific odour-evoked behaviour. Our definition of determinants of Or22a retuning also informs the molecular basis of odour–receptor interactions. When mapped onto a presumed homologous Orco structure<sup>37</sup>, the key change (M93I) falls within a putative ligand-binding pocket, and may be a ‘hotspot’ for functional evolution (Extended Data Fig. 11a–c).

Although functional differences in Or22a are important, they cannot explain the behavioural differences of *D. sechellia* and *D. simulans*, as these receptors are interchangeable for supporting noni attraction. We note that the responses of native Or22a neurons in *D. sechellia* and Or22a/b neurons in *D. simulans* are not identical (Fig. 3a, b); the loss of *Or22b* in *D. sechellia* led to a narrowed (and possibly slightly increased) sensitivity to methyl esters, which could be behaviourally relevant. The expansion of this population of neurons specifically in *D. sechellia* is probably a key additional evolutionary innovation, although alone it is insufficient to restore host attraction similar to that of *D. sechellia* when expressing DmelOr22a. The difference in *D. sechellia* projection neuron axon innervations suggests that changes in central-circuit connectivity form part of the adaptation of this species to noni. Future studies are necessary to understand the genetic bases and behavioural importance of these neuroanatomical differences.

The critical role of Or22a in host attraction in *D. sechellia* may account for the rapid molecular evolution of this locus<sup>38–40</sup> (Extended Data Fig. 11d–h). *Drosophila erecta*—a specialist on *Pandanus* fruit—also exhibits expansion of this OSN population<sup>21</sup>. However, a second noni-adapted drosophilid (*D. yakuba mayottensis*)<sup>41</sup> does not share the receptor or OSN number changes that we describe here (Extended Data Fig. 11i–m) which implies it has developed an independent evolutionary solution to locate a common host fruit.

Finally, other olfactory channels are important for noni attraction. These include Or85c/b neurons (which have conserved physiology but increase in number in *D. sechellia* relative to other drosophilids) and Ir75b neurons, which have both changed in function and number in *D. sechellia* while apparently preserving the anatomy of partner projection neurons<sup>15</sup>. Future application of the *D. sechellia* genetic toolkit should offer further fundamental insights into how genes and neurons control behaviour and enable the evolution of novel traits.

### Online content

Any methods, additional references, Nature Research reporting summaries, source data, extended data, supplementary information, acknowledgements, peer review information; details of author contributions and competing interests; and statements of data and code availability are available at <https://doi.org/10.1038/s41586-020-2073-7>.

1. Arguello, J. R. & Benton, R. Open questions: tackling Darwin's “instincts”: the genetic basis of behavioral evolution. *BMC Biol.* **15**, 26 (2017).
2. Bendsky, A. & Bargmann, C. I. Genetic contributions to behavioural diversity at the gene–environment interface. *Nat. Rev. Genet.* **12**, 809–820 (2011).

3. Bendesky, A. et al. The genetic basis of parental care evolution in monogamous mice. *Nature* **544**, 434–439 (2017).
4. Ding, Y., Berrocal, A., Morita, T., Longden, K. D. & Stern, D. L. Natural courtship song variation caused by an intronic retroelement in an ion channel gene. *Nature* **536**, 329–332 (2016).
5. Weber, J. N., Peterson, B. K. & Hoekstra, H. E. Discrete genetic modules are responsible for complex burrow evolution in *Peromyscus* mice. *Nature* **493**, 402–405 (2013).
6. Garrigan, D. et al. Genome sequencing reveals complex speciation in the *Drosophila simulans* clade. *Genome Res.* **22**, 1499–1511 (2012).
7. Schriber, D. R., Ayroles, J., Matute, D. R. & Kern, A. D. Supervised machine learning reveals introgressed loci in the genomes of *Drosophila simulans* and *D. sechellia*. *PLoS Genet.* **14**, e1007341 (2018).
8. Amlou, M., Moreteau, B. & David, J. R. Genetic analysis of *Drosophila sechellia* specialization: oviposition behavior toward the major aliphatic acids of its host plant. *Behav. Genet.* **28**, 455–464 (1998).
9. Cobb, M., Burnet, B., Blizard, R. & Jallon, J. M. Courtship in *Drosophila sechellia* – its structure, functional aspects, and relationship to those of other members of the *Drosophila melanogaster* species subgroup. *J. Insect Behav.* **2**, 63–89 (1989).
10. Coyne, J. A. Genetics of sexual isolation in females of the *Drosophila simulans* species complex. *Genet. Res.* **60**, 25–31 (1992).
11. Dekker, T., Ibba, I., Siju, K. P., Stensmyr, M. C. & Hansson, B. S. Olfactory shifts parallel superspecialism for toxic fruit in *Drosophila melanogaster* sibling, *D. sechellia*. *Curr. Biol.* **16**, 101–109 (2006).
12. Higa, I. & Fuyama, Y. Genetics of food preference in *Drosophila sechellia*. I. Responses to food attractants. *Genetica* **88**, 129–136 (1993).
13. Ibba, I., Angioy, A. M., Hansson, B. S. & Dekker, T. Macroglomeruli for fruit odors change blend preference in *Drosophila*. *Naturwissenschaften* **97**, 1059–1066 (2010).
14. Matsuo, T., Sugaya, S., Yasukawa, J., Aigaki, T. & Fuyama, Y. Odorant-binding proteins OBP57d and OBP57e affect taste perception and host-plant preference in *Drosophila sechellia*. *PLoS Biol.* **5**, e118 (2007).
15. Prieto-Godino, L. L. et al. Evolution of acid-sensing olfactory circuits in Drosophilids. *Neuron* **93**, 661–676 (2017).
16. R’Kha, S., Capy, P. & David, J. R. Host-plant specialization in the *Drosophila melanogaster* species complex: a physiological, behavioral, and genetical analysis. *Proc. Natl Acad. Sci. USA* **88**, 1835–1839 (1991).
17. Yalcin, B. et al. Genetic dissection of a behavioral quantitative trait locus shows that *Rgs2* modulates anxiety in mice. *Nat. Genet.* **36**, 1197–1202 (2004).
18. Bendesky, A., Tsunozaki, M., Rockman, M. V., Kruglyak, L. & Bargmann, C. I. Catecholamine receptor polymorphisms affect decision-making in *C. elegans*. *Nature* **472**, 313–318 (2011).
19. Bumbarger, D. J., Riebesell, M., Rödelsperger, C. & Sommer, R. J. System-wide rewiring underlies behavioral differences in predatory and bacterial-feeding nematodes. *Cell* **152**, 109–119 (2013).
20. Markow, T. A. & O’Grady, P. Reproductive ecology of *Drosophila*. *Funct. Ecol.* **22**, 747–759 (2008).
21. Linz, J. et al. Host plant-driven sensory specialization in *Drosophila erecta*. *Proc. R. Soc. Lond. B* **280**, 20130626 (2013).
22. Seeholzer, L. F., Seppo, M., Stern, D. L. & Ruta, V. Evolution of a central neural circuit underlies *Drosophila* mate preferences. *Nature* **559**, 564–569 (2018).
23. Dweck, H. K. et al. Olfactory channels associated with the *Drosophila* maxillary palp mediate short- and long-range attraction. *eLife* **5**, e14925 (2016).
24. Matute, D. R. & Ayroles, J. F. Hybridization occurs between *Drosophila simulans* and *D. sechellia* in the Seychelles archipelago. *J. Evol. Biol.* **27**, 1057–1068 (2014).
25. Vosshall, L. B. & Stocker, R. F. Molecular architecture of smell and taste in *Drosophila*. *Annu. Rev. Neurosci.* **30**, 505–533 (2007).
26. Larsson, M. C. et al. *Or83b* encodes a broadly expressed odorant receptor essential for *Drosophila* olfaction. *Neuron* **43**, 703–714 (2004).
27. Abuin, L. et al. Functional architecture of olfactory ionotropic glutamate receptors. *Neuron* **69**, 44–60 (2011).
28. Benton, R., Sachse, S., Michnick, S. W. & Vosshall, L. B. Atypical membrane topology and heteromeric function of *Drosophila* odorant receptors in vivo. *PLoS Biol.* **4**, e20 (2006).
29. Stensmyr, M. C., Dekker, T. & Hansson, B. S. Evolution of the olfactory code in the *Drosophila melanogaster* subgroup. *Proc. R. Soc. Lond. B* **270**, 2333–2340 (2003).
30. Dobritsa, A. A., van der Goes van Naters, W., Warr, C. G., Steinbrecht, R. A. & Carlson, J. R. Integrating the molecular and cellular basis of odor coding in the *Drosophila* antenna. *Neuron* **37**, 827–841 (2003).
31. Couto, A., Alenius, M. & Dickson, B. J. Molecular, anatomical, and functional organization of the *Drosophila* olfactory system. *Curr. Biol.* **15**, 1535–1547 (2005).
32. Shiao, M. S. et al. Expression divergence of chemosensory genes between *Drosophila sechellia* and its sibling species and its implications for host shift. *Genome Biol. Evol.* **7**, 2843–2858 (2015).
33. Yao, C. A., Ignell, R. & Carlson, J. R. Chemosensory coding by neurons in the coeloconic sensilla of the *Drosophila* antenna. *J. Neurosci.* **25**, 8359–8367 (2005).
34. Ai, M. et al. Acid sensing by the *Drosophila* olfactory system. *Nature* **468**, 691–695 (2010).
35. Ruta, V. et al. A dimorphic pheromone circuit in *Drosophila* from sensory input to descending output. *Nature* **468**, 686–690 (2010).
36. Grabe, V. & Sachse, S. Fundamental principles of the olfactory code. *Biosystems* **164**, 94–101 (2018).
37. Butterwick, J. A. et al. Cryo-EM structure of the insect olfactory receptor *Orco*. *Nature* **560**, 447–452 (2018).
38. Aguadé, M. Nucleotide and copy-number polymorphism at the odorant receptor genes *Or22a* and *Or22b* in *Drosophila melanogaster*. *Mol. Biol. Evol.* **26**, 61–70 (2009).
39. Goldman-Huertas, B. et al. Evolution of herbivory in Drosophilidae linked to loss of behaviors, antennal responses, odorant receptors, and ancestral diet. *Proc. Natl Acad. Sci. USA* **112**, 3026–3031 (2015).
40. Nozawa, M. & Nei, M. Evolutionary dynamics of olfactory receptor genes in *Drosophila* species. *Proc. Natl Acad. Sci. USA* **104**, 7122–7127 (2007).
41. Yassin, A. et al. Recurrent specialization on a toxic fruit in an island *Drosophila* population. *Proc. Natl Acad. Sci. USA* **113**, 4771–4776 (2016).

**Publisher’s note** Springer Nature remains neutral with regard to jurisdictional claims in published maps and institutional affiliations.

© The Author(s), under exclusive licence to Springer Nature Limited 2020